Characterization of endothelial cell injury by cholesterol oxidation products found in oxidized LDL

Alex Sevanian, Howard N. Hodis, Juliana Hwang, Laurie L. McLeod, and Hazel Peterson

Department of Molecular Pharmacology and Toxicology, School of Pharmacy, University of Southern California, 1985 Zonal Avenue, Los Angeles, CA 90033

Abstract The present study describes the toxicity of oxidized LDL towards rabbit aortic endothelial cells in terms of its lipid components with specific attention to the cholesterol oxidation products (ChOx) found in oxidized LDL isolated from human plasma. Measurements of the major ChOx associated with freshly isolated unmodified LDL, those found in oxidized LDL isolated from human plasma and LDL subjected to oxidation in vitro are described. We have confirmed previous findings that most of the cytotoxicity of freshly isolated human LDL may be attributable to a minor fraction that appears to be oxidatively modified by several criteria. Moreover, this plasma-derived oxidized LDL (referred to as LDL⁻) is highly enriched in ChOx, whereas the content of lipid peroxides or derived products (measured as conjugated dienes and thiobarbituric acid reacting products) are much lower, particularly when compared to copper-induced LDL oxidation. Much of the ChOx found in plasma are associated with LDL⁻, however, the levels and proportions of the various ChOx found in LDL⁻ differ from those produced after extensive copper-induced oxidation but resemble those produced after moderate oxidation with copper. The species and concentrations of ChOx found in LDL⁻ when applied as a mixture exhibit considerably more toxicity than any individual ChOx alone. At non-toxic levels this ChOx mixture causes an increased influx of several ions, including calcium, an effect not seen with individual ChOx at comparable doses. Perturbations in ionic homeostasis, and particularly the sustained increase in intracellular calcium concentrations, are associated with much of the cytotoxicity, an effect attributable to the membrane disruptive action of ChOx leading to altered ion transporter activity. The effect of the ChOx mixture (but not any individual ChOx) on sodium and potassium flux appears to be due to enhanced Na^+/K^+-ATPase activity based on the complete inhibition produced by ouabain under all treatment conditions. These findings also show that the levels of cholesterol oxidation products found in normal LDL are not cytotoxic whereas those present in oxidized LDL exceed the toxic threshold for endothelial cells and account for most of the cytotoxicity produced by this modified lipoprotein.—**Sevanian, A., H. N. Hodis, J. Hwang, L. L. McLeod, and H. Peterson.** Characterization of endothelial cell injury by cholesterol oxidation products found in oxidized LDL. *J. Lipid Res.* 1995. **36:** 1971–1986.

Supplementary key words atherosclerosis • LDL oxidation • oxysterols • sodium • potassium • calcium • ionic homeostasis

Oxidative modification of low density lipoproteins (LDL) is widely regarded as a contributing process in the development of atherosclerosis. Oxidation of LDL increases the cytotoxicity and atherogenicity of this particle (1). Both oxidatively modified LDL and cholesterol oxidation products (ChOx) are found in atherosclerotic lesions (2, 3) and in the plasma (4, 5), and their levels appear related to lipoprotein cholesterol levels. Similar forms of oxidized LDL are produced by cell-mediated as well as metal- and oxidant-catalyzed reactions (6–8). Oxidatively modified LDL prepared by these methods is considerably more cytotoxic than unmodified LDL (1), contains substantial amounts of ChOx (9), and elicits a variety of vascular cell responses that reflect early events during atherogenesis. Representative effects include induction of cytokines (10), stimulation of monocyte adhesion and chemotaxis (11), and increased cellular LDL-cholesterol uptake and lipid loading of macrophages (1).

Increased plasma levels of LDL are considered as a risk factor for atherosclerosis. There are numerous reports that high levels of LDL-cholesterol are injurious to the endothelium. Adverse effects include perturbations in the formation of vasoactive agents with consequent loss of vascular tone regulation (12) and stimulation of oxyradical formation (13). Enhanced production of oxidizing agents by vascular tissues or resident inflammatory cells may be responsible for the formation of oxidatively modified LDL found in vivo (1, 14). Accordingly, the ability to produce oxidized LDL may

Abbreviations: ChOx, cholesterol oxidation products; LDL, low density lipoprotein; LDL⁻, oxidized LDL; n-LDL, unmodified LDL; HPLC, high performance liquid chromatography; PBS, phosphate-buffered saline; TMS, trimethylsilyl; REC, rabbit aortic endothelial cells; FBS, fetal bovine serum; LPDS, lipoprotein-deficient serum; 7α-OH, 5-cholestene-3β,7α-diol; 7β-OH, 5-cholestene-3β,,7β-diol; α-epox, cholestan-5α,6α-epoxy-3β-ol; β-epox, cholestan-5β,6β-epoxy-3β-ol; CT, cholestan-3β,5α,6β-triol; 7-keto, 5-cholesten-3β-ol-7-one; 25-OH, 5-cholesten-3β,25-diol.

be augmented via elevated LDL which both stimulates oxidation and acts as the enlarged target for the processes that lead to its oxidation. Previous studies have described elevated plasma levels of a modified LDL (referred to as LDL⁻ in this report) in hypercholesterolemic humans (15) and animals (16). Moreover, the LDL⁻ is enriched in lipid peroxidation products and is more electronegative than normal LDL based on its anion exchange high pressure liquid chromatography (HPLC) and gel electrophoresis characteristics (15, 16). The increased oxidation is accompanied by increased levels of ChOx that are largely associated with LDL (17), and particularly enriched in the LDL⁻ fraction (16).

LDL⁻ recovered from hypercholesterolemic animals is highly cytotoxic to endothelial cells whereas comparable or greater amounts of unoxidized LDL are not toxic (16). Recent studies suggest that much of the cytotoxicity of oxidized LDL is associated with the ChOx (18) which appear to be formed by gradual oxidation of the lipoprotein in vivo. This is suggested by several in vivo (19, 20) and in vitro (21, 22) studies demonstrating the cytotoxicity of ChOx found in LDL and their role in atherosclerotic-type lesion formation. The cytotoxicity of ChOx may manifest by a number of mechanisms and the effects on cell membranes have been well documented (23). A possible consequence of membrane disruption is perturbation of enzymes involved in ion transport. ChOx have been shown to affect Na^+, K^+, and Ca^{2+} flux where, for example, cholestan-3β,5α,6β-triol, 25-hydroxycholesterol, and 7-ketocholesterol enhanced Na^+/K^+-ATPase activity in fibroblasts and smooth muscle cells (24, 25). Stimulation of Ca^{2+} influx has also been reported after treatments with the above-mentioned as well as other ChOx (26). In this report, we describe further the cytotoxicity of in vivo oxidized LDL (i.e., LDL⁻) based on its enriched ChOx content from the standpoint of the types of ChOx found in this lipoprotein. A range of ChOx concentrations, including those found in LDL⁻, were used to assess cytotoxicity towards endothelial cells as well as effects on ion flux in comparison to the effects of LDL⁻, normal LDL, and Cu^{2+}-oxidized LDL.

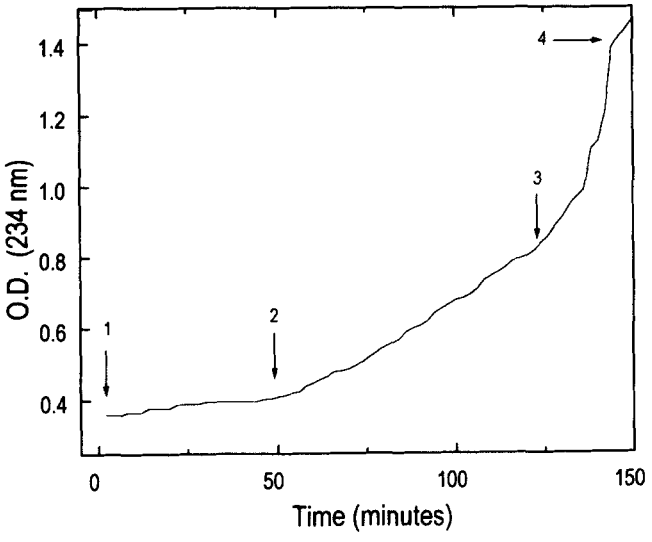

Fig. 1. A representative tracing for the progression of LDL oxidation is shown. Freshly isolated LDL was pipetted into a spectrophotometric cuvette containing phosphate-buffered saline. The amount of LDL in each sample was adjusted to a final protein concentration of 500 μg/mL. Oxidation was initiated by addition of 10 μM (final) $CuSO_4$ (prepared in water). The progress of oxidation was then continuously monitored at 234 nm, and when desired, the sample was recovered for further use or analysis as described in the text. Arrow no. 1 represents the zero time point or the background level of peroxidation in the LDL sample. Arrow no. 2 shows the typical end of the oxidation lag phase when LDL is minimally oxidized. Arrow no. 3 indicates the mid-point of the propagation phase for LDL lipid peroxidation. Samples were recovered at this point for analysis of lipid peroxidation products or for cytotoxicity experiments. Arrow no. 4 indicates the time when LDL oxidation is nearly maximum and termination reactions prevail.

METHODS

Materials

Cholesterol oxides were purchased from Steraloids, Inc. (Wilton, NH). The following reagents were obtained from Sigma Chemical Co. (St. Louis, MO): $MnCl_2$, $CaCl_2$, ethyleneglycol-bis-(β-amino-ethyl ether) N,N′-tetraacetic acid (EGTA), bradykinin, ionomycin, ouabain, amiloride, and HEPES buffer. A23187, Fluo3-AM, and 1,2 bis[2-aminophenoxy]-ethane-N,N,N,N-tetraacetic acid (BAPTA-AM) were obtained from Molecular Probes, Inc. (Eugene, OR). All cell culture media were obtained from Gibco, Grand Island, NY and fetal bovine serum was from Gemini Bioproducts, Calabasas, CA. Endothelial cell growth factor and gentamicin were purchased from Sigma, Inc., St. Louis, MO. [U-^{14}C]*l*-Leucine, ^{86}Rb, and ^{22}Na were obtained from Amersham, Arlington Heights, IL. All organic solvents were HPLC grade and purchased from J. T. Baker Chemical Co. (Phillipsburg, NJ).

Isolation of LDL from plasma

Venous blood was obtained from fasting adult human volunteers with total plasma cholesterol levels ranging from 160 to 210 mg/dL. Blood was collected into 10-mL Vacutainer tubes containing EDTA where the final EDTA concentration was 1 mg/mL blood. Plasma was immediately separated by centrifugation at 1500 *g* for 10 min at 4°C. LDL (δ 1.019–1.063 g/mL) was separated from freshly drawn plasma by preparative ultracentrifugation with a Beckman L8-55 ultracentrifuge equipped with an SW-41 rotor as described previously (16). After separation, the LDL was dialyzed against

argon-sparged 0.01 M Tris-HCl buffer, pH 7.2, containing 50 μM EDTA. Cholesterol levels were measured enzymatically using a VP Super System instrument (Abbott, Dallas, TX) according to Lipid Research Clinic methodology (27). The isolated LDL was kept in argon-sparged buffer at 4°C for no more than 24 h before further processing as described below.

Preparation of LDL⁻

Separation of LDL⁻ from unmodified LDL was accomplished using anion exchange high performance liquid chromatography (HPLC) (Perkin Elmer Series 4 HPLC) as described previously (16). The eluent was monitored at 280 nm and peaks corresponding to unmodified or normal LDL (n-LDL) and LDL⁻ were collected in 1-mL aliquots using a fraction collector. The amount of LDL protein was determined for each peak using the method of Lowry et al. (28) and used for peak area calibration from which the amounts of n-LDL and LDL⁻ were routinely computed. Fractions were collected into tubes containing 50 μM EDTA in 0.01 M Tris-HCl buffer, pH 7.2, and those fractions containing LDL⁻ were pooled, concentrated, and all salts removed by centrifugation with Centricon 10,000 molecular weight microconcentrators (Beverly, MA). This procedure causes minimal LDL aggregation which is indistinguishable from that produced by conventional dialysis. Samples were diluted in phosphate-buffered saline, the protein content was determined, and the samples were then used for the various studies described below and aliquots were extracted for determinations of ChOx content as detailed below.

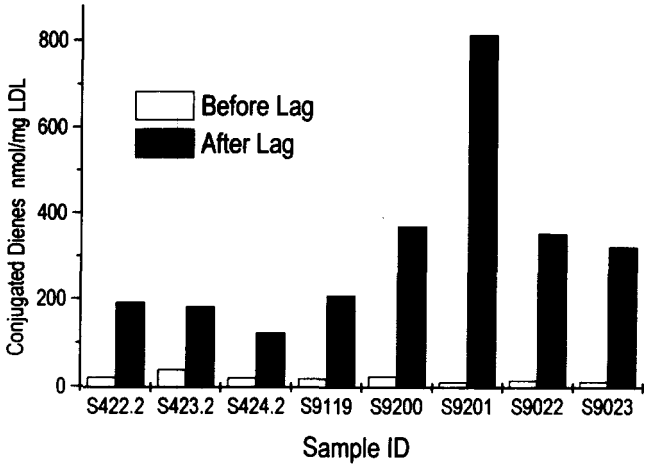

Fig. 2. The content of conjugated dienes in eight representative preparations of LDL from different donors immediately after isolation. The samples are identified by the laboratory identification number. As indicated in the inset, Before Lag corresponds to arrow 1 shown in Fig. 1. Also shown are the levels of conjugated dienes formed after subjecting the sample to Cu^{2+}-induced oxidation to the extent indicated by arrow 3 in Fig. 1 and referred to as After Lag in the inset.

In vitro oxidation of LDL

Fresh preparations of LDL were subjected to oxidation as follows. Samples of LDL were mixed and incubated with 10 μM $CuSO_4$ in phosphate-buffered saline (PBS) at 22°C for intervals of up to 6 h. The reaction was monitored continuously at 234 nm with a Beckman DU650 spectrophotometer and Beckman proprietary spectrophotometric software in 1-mL quartz cuvettes containing 500 μg LDL protein. As the rate and extent of LDL oxidation varies among samples from different donors, the degree of oxidation was determined by continuously measuring the increase in conjugated dienes (OD = 234 nm) over the incubation interval. This spectrophotometric assay was based on the method of Esterbauer et al. (29), enabling measurement of the oxidative lag phase (recorded in minutes) and the rate of peroxidation during the propagation phase. The level of total peroxides in LDL was estimated using a molar extinction coefficient of 2.54×10^4 for lipid-conjugated dienes measured at the end of the incubation period. After oxidation, LDL was collected and dialyzed by two successive centrifugations with Centricon 10,000 molecular weight microconcentrators. These preparations were then adjusted to desired concentrations for analysis of LDL⁻ content by HPLC, as described above, or used for other analyses as reported below.

Measurements of LDL oxidation

The progress of LDL oxidation was determined either directly by monitoring formation of conjugated dienes in LDL suspensions via the absorbance change at 234 nm, or by measurement of conjugated dienes on lipid extracts of LDL using second derivative spectroscopy as described previously (30). For the latter measurements, samples of LDL containing 500 μg protein per mL were extracted with 6 mL chloroform–methanol 2:1 after various periods of incubation with the oxidizing system. The organic phase was collected and saved, and the aqueous phase was re-extracted with another 3 mL chloroform–methanol 2:1 and the organic phases were pooled. After evaporation of the organic solvent under a stream of nitrogen at room temperature, the lipid residue was redissolved in absolute ethanol and the absorbance was monitored over the frequency range of 220–300 nm against an ethanol blank. The extent of peroxidation was estimated from the sum of the absorbance minima at 242 and 233 nm corresponding to the *cis/trans* and *trans/trans* diene conjugate isomers. Linoleic acid hydroperoxide, prepared as described previously (31), was used to develop a calibration curve. All scans were taken with a Beckman DU650 spectrophotometer. The content of lipid peroxides was estimated from the total *cis/trans* and *trans/trans* conju-

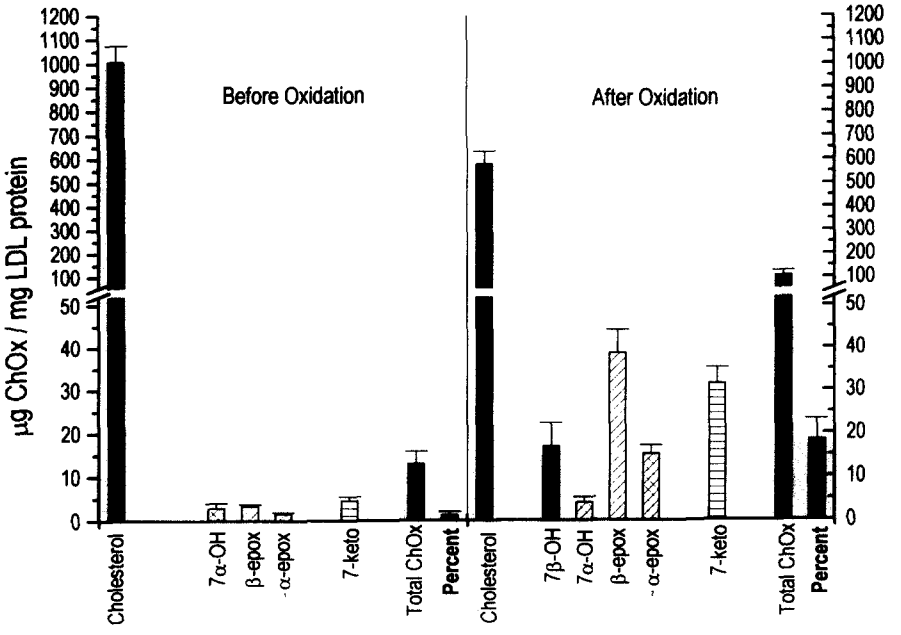

Fig. 3. The contents of cholesterol oxidation products (ChOx) measurable by gas chromatography are shown before oxidation of LDL (represented by arrow 1 in Fig. 1) and after Cu^{2+}-induced oxidation to an extent represented by arrow 3 in Fig. 1. The lipid peroxide content (estimated by conjugated dienes measured by second derivative UV spectroscopy of lipid extracts) was 31 ± 11 nmol/mg LDL protein before oxidation and 222 ± 79 nmol/mg LDL protein after oxidation. The amounts of each ChOx as well as the total ChOx are shown as well as the amount of total ChOx expressed as a percent of the cholesterol content in the sample. Values for samples before oxidation are derived from nine independent analyses while those for samples after oxidation are from five independent analyses.

gated dienes using and a molar extinction coefficient of 2.54×10^4.

Measurement of ChOx

Characterization and quantitation of ChOx was performed as described previously (17, 32). Briefly, sample aliquots containing approximately 0.5 mg LDL protein were immediately purged with argon after isolation or after various periods of oxidation, as described above. The sample was sealed under an argon atmosphere and stored at -70°C for no longer than 1 week before being analyzed. Lipids were extracted with chloroform–methanol 2:1 (v/v) containing 0.01% BHT. An internal standard (5α-cholestane, 100 µL @ 10 µg/uL) was added to each sample at the time of extraction. The lipid extract was evaporated to dryness under nitrogen and the residue was dissolved in 1.0 mL toluene–ethyl acetate 1:1 (v/v). The neutral lipid fraction, containing cholesterol and ChOx, and the phospholipids (polar lipid fraction) were isolated by sequential elution of solid phase extraction columns with toluene–ethyl acetate followed by methanol (Bakerbond Diol columns, J. T. Baker, Inc. Phillipsburg, NJ). The phospholipids were saved frozen under nitrogen while aliquots of the neutral lipid fraction were subjected to mild alkaline saponification followed by treatment with ethereal diazomethane. The sample was then transferred into a 1.0-mL autoinjector vial and lipids were converted to trimethylsilyl (TMS) ethers using dimethylformamide and N,O-*bis*(trimethylsilyl) trifluoroacetamide (BSTFA, Supelco, Inc., Bellefonte, PA) (1:1 v/v). The vials were sealed, purged with argon, heated at 80°C for 30 min and injected into a Shimadzu GC-14A gas chromatograph. A description of the chromatographic conditions can be found elsewhere (17). Quantitative analysis of biological samples was performed by the internal standard method. A set of standards corresponding to common ChOx previously identified in human plasma were analyzed under the same conditions in order to verify the identity of ChOx found in LDL.

Cytotoxicity assays

Rabbit aortic endothelial cells (REC) were isolated from New Zealand albino rabbits and used between passages 9 and 13. The characteristics of these cells have been described elsewhere (21). Cells were grown in 6- or 12-well dishes and maintained in complete medium consisting of DMEM–M199 80:20 with 10% fetal bovine serum (FBS), endothelial cell growth factor (5 µg/mL), and gentamicin (50 µg/mL). Conditioned medium was

added at the time of medium change at a 1:4 ratio with fresh medium. The phenotype of the cells was checked on the basis of the expression of factor VIII antigen, angiotensin converting enzyme activity, and by morphological characteristics. Stock cells were passaged using a 1:3 split ratio with mechanical disruption of the monolayer. Cultures were maintained with weekly media changes. Freshly isolated LDL⁻ or n-LDL was added to subconfluent cultures (5×10^5 cells/well) over a range of treatment concentrations and measurement of toxicity was performed by determining the surviving fraction of cells after 24 h as described previously (16). The treatment concentrations are expressed as serum equivalents where, for example, a 10% serum equivalent dose corresponds to 10% of the lipoproteins present in serum. The 10% serum equivalent is generally the serum concentration (10% FBS) in complete cell culture medium. Similarly, a ChOx mixture, representative of the major ChOx present in LDL⁻, was added to selected cultures in a manner analogous to LDL treatments; however, ChOx were added to the medium using an ethanol vehicle where the final ethanol concentration was ≤ 0.5% (v/v). The composition of the ChOx mixture and amounts [expressed as mole fraction × 100] of each component were as follows: 5-cholestene-3β,7α-diol [10.2] (7α-OH), 5-cholestene-3β,7β-diol [6.7] (7β-OH), cholestan-5α,6α -epoxy-3β-ol [10.3] (α-epox), cholestan-5β,6β-epoxy-3β-ol [24.3] (β-epox), cholestan-3β,5α,6β-triol [10.0] (CT), 5-cholesten-3β-ol-7-one [31.0] (7-keto), and 5-cholesten-3β,25-diol [7.3] (25-OH), approximating the proportions of ChOx found in LDL⁻. The mixture was added over a range of concentrations representative of that found in human LDL⁻ or from hypercholesterolemic monkeys (16) and expressed as percent serum equivalent concentrations in complete medium.

In addition to the above determinations, acute toxicity was measured by means of [^{14}C]leucine release from REC into the medium. This provided a measure of cell injury in terms of damage to cell membranes and leakage of peptides and proteins. Subconfluent cultures of REC were incubated with [^{14}C]leucine for 48 h at 1.0 μCi/well in complete medium. Prior to treatment, the cells were washed three times with complete medium and then incubated with the ChOx mixture in media containing 2% LDL-deficient FBS (LPDS) for 2 h. Addition of complete medium containing undetectable levels of ChOx to selected wells provided an estimate of the background (control) rate of radioactivity released by cells. After incubation, aliquots of the medium were treated with 12% cold TCA (final concentration), the precipitates were washed, and their radioactivity content was measured in a Beckman LS-7500 scintillation counter. The level of radioactivity in the precipitates is expressed as a percentage of radiolabel released from untreated (control) cultures.

Measurements of ionic flux

The effects of n-LDL, LDL⁻, and ChOx on the influx or efflux of Na^+, K^+, and Ca^{2+} were determined in parallel with cytotoxicity measurements. Subconfluent cultures similar to that described above were used for measurements of Na^+ influx. Treatment with the ChOx was for 2 h in 2% LPDS media after which the monolayers were washed three times with Na^+-free choline-buffer (choline chloride, 100 mM; magnesium chloride, 30 mM; potassium chloride, 3 mM, pH 7.4) to remove excess Na^+. The monolayers were allowed to equilibrate for 10 min at 37°C. Choline-buffer containing $^{22}Na^+$ at 10^5 dpm/well (sp act, 90 mmol/mCi, NEN, Wilmington, DE) was added to the wells and at designated time periods up to 5 min the monolayers were washed with PBS (containing excess cold Na^+), trypsinized, and counted for cell number and radioactivity. Measurements of ouabain-resistant Na^+ and K^+ influx were made in the presence of 1 mM ouabain final concentration,

TABLE 1.

	Cholesterol[a]	ChOx as % of Cholesterol[b]	TBAR[c]
	mg/dL		nmol/mg LDL-*C*
nLDL	108 ± 8.3	2.2 ± 1.2	1.2 ± 0.03
LDL⁻	2.4 ± 0.5	29.6 ± 9.1	4.6 ± 1.1
Oxid. nLDL[d]	88 ± 9.0	31.4 ± 9.3	39.3 ± 6.9

[a]Total cholesterol in lipoproteins was measured by gas chromatography as described in Methods.

[b]ChOx in lipoproteins was measured by gas chromatography as described in Methods and is expressed as a percentage of cholesterol in the lipoprotein using the sum of the ChOx measurements.

[c]TBAR for each lipoprotein was measured as described in Methods and is expressed as nmol/mg LDL⁻ cholesterol using a molar extinction coefficient of 5.6×10^5 for malondialdehyde and cholesterol levels were measured as described in *a*.

[d]nLDL after isolation by anion exchange HPLC was incubated with 10 μM $CuSO_4$ in phosphate-buffered saline for intervals sufficient to induce propagation of lipid peroxidation. The LDL was recovered at the mid-point of the propagation phase as indicated by arrow 3 in Fig. 1, and the ChOx was extracted for GC analysis.

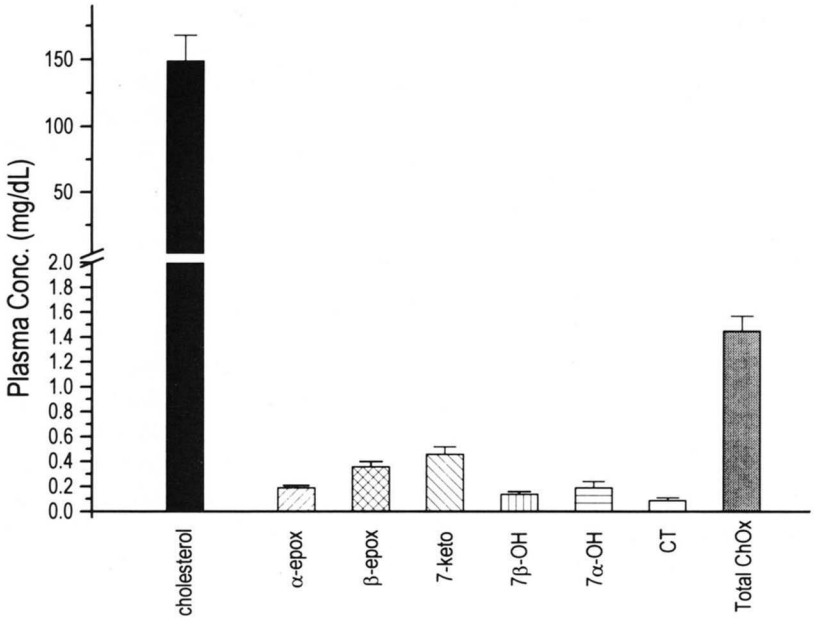

Fig. 4. The content of the major ChOx recovered from human plasma. All ChOx were characterized and quantitated by gas chromatography and values are expressed as mg/dL plasma. Total ChOx represents the sum of the individual ChOx expressed as a percent of the plasma total cholesterol also measured by gas chromatography. Results, expressed as mean and standard error, are from the analysis of eight plasma samples obtained from different donors.

which was added to the choline-buffer 2 min prior to addition of $^{22}Na^+$ or ^{86}Rb. Measurements of Na^+ efflux were made after prelabeling REC with $^{22}Na^+$ for 18 h (0.1 μCi/mL in complete medium) prior to addition of ChOx. Treatment with the ChOx was for 2 h in 2% LPDS media after which the monolayers were washed three times with Na^+-free choline-buffer (choline chloride, 100 mM; magnesium chloride, 30 mM; potassium chloride, 3 mM, pH 7.4) to remove excess Na^+. The monolayers were allowed to equilibrate for 10 min at 37°C. Choline-buffer was added to the wells and at designated time periods up to 5 min aliquots of the medium were taken for measurement of radioactivity. The monolayers were then washed with PBS (containing excess cold Na^+), trypsinized, and counted for cell number and radioactivity. Ouabain (1 mM) was also present in some wells during the last 2 h to determine the extent of ouabain-sensitive Na^+ (or K^+, see below) flux. Measurements of cell number and cell associated radioactivity were made at the end of the designated time intervals.

Measurements of K^+ uptake were made utilizing ^{86}Rb as a radiotracer. For these studies, REC were grown to the required density in 24-well plates. The uptake of ^{86}Rb was determined over a 2-h period concurrent with the treatment of the monolayers with the ChOx mixture in DMEM/M199 (4:1) and [^{86}Rb]Cl, 1 μCi/ml, (sp act, 4.6 mCi/mmol) containing 2% FBS. At the end of treatment, the media was removed and the monolayers were washed three times with PBS containing excess K^+, trypsinized, and counted for cell number and radioactivity. The extent of ^{86}Rb uptake over the fixed 2-h interval was used to estimate rates of K^+ uptake which is expressed as a percentage of the rate found in untreated (control) cells.

Intracellular free calcium concentrations ($[Ca^{2+}]_i$) were measured fluorometrically using a Hitachi F-2000 fluorometer. REC grown directly on polymethacrylate fluorometer cuvettes (Sigma, St. Louis, MO) in 1 mL complete media buffered with 10 mM HEPES were loaded with the fluorescent probe, fluo-3-AM by adding 5 μL of a 1 mM solution in DMSO directly to cuvettes resulting in a final probe concentration of 5 μM. The cultures were left for up to 1 h at 21°C and uptake and completeness of ester hydrolysis were monitored by measuring the fluorescence intensity signal over this interval. This served to establish the optimum cell loading time. The fluorescence signal was found to reach a maximum that stabilized in about 45–60 min after addition of the probe. Unincorporated probe was removed from the cells by two washings, first with fresh media, then with the Ca^{2+}-free HEPES buffer (10 mM). ChOx, prepared in complete medium containing 2% FBS, were added to the cells after labeling with the probe and the change in Ca^{2+} levels was monitored over the time. The fluorescence emission signal at 526 nm was collected at a right angle from the excitation beam. A 0.1- to 2-sec response time and a 150 watt xenon lamp at 400V was used to deliver 506 nm excitation beam through a grating monochrometer to the sample compartment containing cells loaded with the fluorescent probe. The excitation and emission band-pass were set to 10 nm. nLDL, LDL$^-$, or ChOx were added to the cuvettes while monitoring the fluorescence. After each experiment, a calibration of the signal was performed. This fluores-

cence signal was converted to Ca^{2+} concentration according to the method of Tsien and Pozzan (33). Briefly, this method involves determining the dye fluorescence at two points within the linear region of the calibration curve: F_{min} (the fluorescence of the unchelated dye) and F_{max} (the fluorescence of the fully chelated dye). This type of calibration was done for each experiment, as the number of cells analyzed and the amount of dye taken up by the cells varied between experiments. Determination of F_{Mn} was accomplished by saturating the dye with Mn (2 mM) after addition of the ionophores A23187 or ionomycin. The signal intensity observed, F_{Mn}, was then used to calculate F_{max} using the following equation:

$$F_{max} = 5 \times (F_{Mn} - F_{bkg}) + F_{bkg}$$

where F_{bkg} is the autofluorescence of the cells without dye which was measured in each instance before addition of the probe, in the absence and presence of ChOx.

This background intensity, F_{bkg}, was also used to determine F_{min}, the minimum dye fluorescence intensity:

$$F_{min} = (F_{max} - F_{bkg})/40 + F_{bkg}$$

The fluorescence intensity signal, F, was converted to $[Ca^{2+}]_i$ using the following equation:

$$[Ca^{2+}]_i = K_d (F - F_{min})/(F_{max} - F)$$

where K_d (400 nM) is the known dissociation constant of the fluo-3 dye/Ca^{2+} complex.

Statistical analyses

The data are expressed as the mean ± standard error calculated from three to five independent experiments, each measurement performed in duplicate. Data for specific treatment groups were subjected to analysis of variance (ANOVA) or the Student's *t*-test.

RESULTS

The kinetic profile for oxidation of freshly isolated LDL in the presence of 10 μM $CuSO_4$ is shown in Fig. 1. The net formation of conjugated dienes in most of the LDL samples analyzed was typical of that shown in Fig. 1. The lag phase prior to the propagation of lipid peroxidation is indicated, as are intervals (indicated by arrows) at which aliquots were taken for measurement of oxidation products during either the lag or propagation phase. The oxidative lag phase varied from 28 to 65 min for the LDL samples analyzed in this study. Considerable differences in the oxidative susceptibility of LDL among subjects have been reported and attributed to the antioxidant content (34) as well as composition and structural variability (35) of the lipoprotein.

Figure 2 shows the level of lipid peroxides measured via second derivative UV spectroscopy of the total lipid extracts taken from samples at zero time (arrow 1) and at the mid-point of the propagation phase (arrow 3). These samples were from eight subjects representing the range of values found in our study and are indicated by their laboratory identification numbers. Small but variable amounts of total conjugated dienes were measured at zero time, estimated to be 31 ± 11 nmol/mg LDL. The LDL samples experienced variable degrees of oxidation where the levels of conjugated dienes ranged from 120 to 800 nmol/mg LDL. No relationship was evident between the levels of conjugated dienes present before oxidation and the levels of conjugated dienes formed after Cu^{2+}-induced oxidation. Moreover, the wide range found for LDL oxidation reflects the disparity in oxidative resistance reported among normal individuals (34). The corresponding levels of ChOx in the

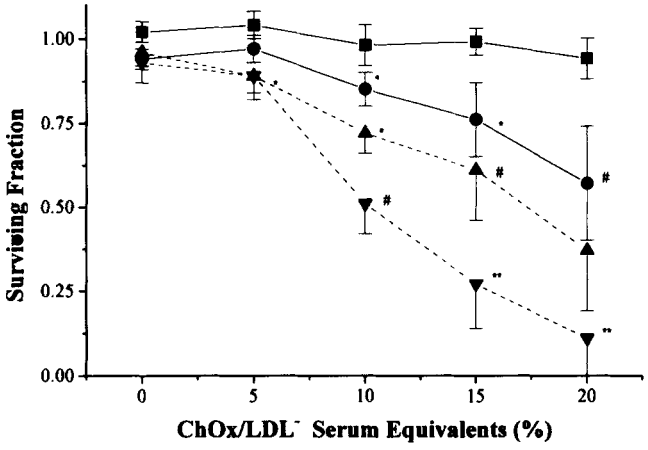

Fig. 5. The cytotoxicities of nLDL (■—■), LDL (▲—▲), Cu^{2+}-oxidized LDL (▼—▼), and ChOx (●—●) are shown. In each instance REC were incubated for 24 h in DMEM-M199 80:20 containing 2% heat-inactivated FBS, which is the minimum serum required to maintain viability over the test period. The medium was prepared with the LDLs or ChOx and was formulated to contain these components at levels that would be present in the indicated equivalent concentrations of serum. For example, a 20% serum equivalent dose contains LDL that would be present in medium that contained 20% serum (assuming that pure serum contains 100 mg/dL LDL). As shown in Fig. 4, ChOx comprise on the average 1% of the plasma total cholesterol. Thus, using an average plasma cholesterol level of 150 mg/dL, a 20% serum equivalent dose represents the addition of 0.30 mg/dL ChOx. ChOx were added in ethanol vehicle (0.2% v/v, ethanol–medium) and control cultures received ethanol only. After treatment, cells were washed and replated in complete medium and the surviving fraction was determined via plating efficiency measured after 24 h of culture. The surviving fraction was calculated from the survival of control cultures that were subjected to the same conditions of culture during treatment and subsequent growth and were assigned a value of 100%. Data points represent the mean and standard error calculated from three independent experiments with each treatment dose measured in duplicate. Determinations of statistical significance were made using a two-tailed *t*-test comparing the log of the surviving fraction for the ChOx/LDL at each treatment dose to untreated control cultures. *, $P < 0.05$, compared to untreated controls; #, $P < 0.01$, compared to untreated controls; **, $P < 0.001$, compared to untreated controls.

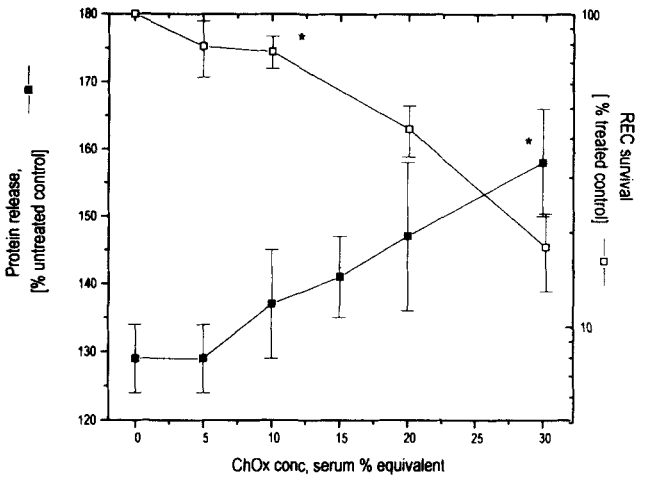

Fig. 6. Release of radiolabeled protein from REC after treatment with the ChOx mixture at the indicated treatment concentrations. As shown in Fig. 4, the ChOx mixture comprises in total approximately 1% of the plasma total cholesterol. Thus, using an average plasma cholesterol level of 150 mg/dL, each 5% serum equivalent incremental dose corresponds to the addition of 0.075 mg/dL ChOx as a mixture. Subconfluent cultures of REC were incubated with [^{14}C]leucine for 48 h at 1.0 μCi/well in complete medium. Prior to treatment, the cells were washed and then incubated with the ChOx mixture in media containing 2% LPDS for 2 h. Addition of complete medium containing undetectable levels of ChOx to selected wells provided an estimate of the background (control) rate of radioactivity released by cells. After a 2-h interval, aliquots of the medium were treated with 12% cold TCA (final concentration), and radioactivity in the washed precipitates was measured. The level of radioactivity in the precipitates was corrected for the total ^{14}C radioactivity associated with cells in each culture and the results are expressed as a percent of radiolabel released from untreated (control) cultures. Also shown are the surviving fractions of treated cells (REC Survival, expressed as the log percent surviving fraction) which were determined concurrently with measurements of radiolabel release. Results are the mean and standard error from three independent analyses. Determinations of statistical significance were made using a two-tailed *t*-test of the log values for each treatment condition (serum equivalent dose) versus the corresponding control values (no ChOx addition) and significant differences ($P < 0.05$) are indicated by asterisks.

LDL before and after oxidation are shown in **Fig. 3.** ChOx identified in freshly isolated LDL not subjected to peroxidation included small amounts of 7α-OH, β-epox, and 7-keto with either trace or undetectable levels of the other oxidation products. After oxidation, the levels of several ChOx increased markedly, among which increases in β-epox and 7β-OH were most evident. The accumulation of ChOx was most evident when expressed as a percentage of the cholesterol in the lipoprotein (far right bar in each panel of Fig. 3). The approximately 10-fold increase in conjugated dienes after Cu^{2+}-induced oxidation was accompanied by about a 15-fold increase in ChOx levels. The greater apparent susceptibility of cholesterol to oxidation and accumulation of ChOx may be due to its participation in chain termination reactions resulting in cholesterol oxidation in lieu of peroxidation of other LDL lipids. The "antioxidant" behavior of cholesterol has been described for various lipid systems (36).

We previously reported that the levels of lipid peroxidation products were elevated in LDL$^-$ as compared to unmodified LDL (nLDL) (15, 16). **Table 1** compares the levels of lipid peroxidation products in nLDL, LDL$^-$, and in Cu^{2+}-oxidized LDL. LDL$^-$ is highly enriched in ChOx, and Cu^{2+}-induced oxidation of freshly isolated nLDL to the extent shown in Fig. 1 (arrow 3, approximately 2 h) resulted in the formation of ChOx to levels comparable to those found in LDL$^-$. However, it is important to note that whereas TBARs also accumulate after oxidation with Cu^{2+}, the content of TBARs in LDL$^-$ is relatively small.

For comparison to the data presented in Fig. 3, **Fig. 4** shows the levels of ChOx measured in human plasma. In this case, the levels of ChOx that would exist in all serum lipoproteins were determined, which fully represents the total ChOx in the circulation to which vascular endothelial cells are potentially exposed. In this case, approximately 1% of the total cholesterol was in the form of ChOx, with β-epox and 7-keto being the major components. β-Epox and 7-keto are also the major ChOx in freshly isolated LDL as well as in Cu^{2+}-oxidized LDL. β-Epox appears to be a predominant cholesterol oxidation product from free radical-mediated oxidation of LDL-cholesterol and the major product found in experimental atherosclerosis (16, 17, 32).

The composition of ChOx found in plasma and LDL$^-$ (16) and, with minor variations, the similar profiles obtained after Cu^{2+}-induced oxidation of LDL afforded formulation of a ChOx mixture representative of the composition of ChOx found in plasma that can be used for cell culture studies. The cytotoxicity of the ChOx mixture was the focus of those studies that drew upon previous characterization of the cytotoxic effects of individual cholesterol oxidation products on vascular cells (16, 19–22). **Figure 5** compares the cytotoxicity of the ChOx mixture to that of LDL$^-$, Cu^{2+}-oxidized LDL, and nLDL. The treatment concentrations are expressed as percent serum equivalents where the serum equivalent dose corresponds to the percentage of the lipoprotein cholesterol that typically exists in complete serum (i.e., we assume that the average LDL-cholesterol is 120 mg/dL). There was no apparent toxicity when cells were treated with nLDL up to a serum equivalent dose of 20% (the maximum level of serum used to culture of REC and equivalent to 0.3 mg/dL of ChOx). On the other hand, 24-h treatments with 10% serum equivalents of LDL$^-$ produced a 30% reduction in the surviving fraction of cells compared to control cultures and a 75% reduc-

tion at 20% serum equivalent doses. Twenty four-h treatments with the ChOx mixture produced a dose-dependent toxicity profile similar to that of LDL, with a 55% decrease in survival using a 20% serum equivalent dose. Treatments with Cu^{2+}-oxidized LDL produced the greatest toxicity where the LDL_{50} dose was 10% serum equivalents under these assay conditions. Comparison of the toxicity curves indicates that the ChOx mixture accounts for most of the cytotoxicity of LDL but not of Cu^{2+}-oxidized LDL. The toxicity of Cu^{2+}-oxidized LDL may be attributed to a number of oxidation products that are found only in minute quantities in in vivo oxidized LDL. Thus, Cu^{2+}-oxidized LDL has, in addition to ChOx, substantial amounts of lipid peroxides and aldehydic decomposition products, as shown in Table 1 and Fig. 2, and reported in previous studies (6), that can contribute to toxicity. It should be noted that the cytotoxic component of oxidized LDL was previously shown to be associated with the neutral lipid fraction (7) where the ChOx are found.

The results of cytotoxicity experiments utilizing measurements of [^{14}C]leucine release from REC are presented in **Fig. 6.** Treatment of [^{14}C]leucine prelabeled cells with the ChOx mixture at serum equivalent doses up to 30% produced an incremental increase in the level of ^{14}C-labeled protein release. For these experiments all ChOx treatments were made in 2% serum-containing medium to minimize the effects of serum factors (particularly the ChOx that may exist in serum) on cell permeability. The level of protein leakage was approximately 20% greater in 2% serum-containing medium as compared to standard culture conditions (i.e., 10% serum-containing medium) where no leakage was measurable over a 2-h period. An apparent threshold was found at a 10% serum equivalent dose of ChOx where leakage of protein increased to approximately 140% of the 2% serum control levels. At 30% serum equivalents, there was a 160% increase in leakage of [^{14}C]leucine-derived radioactivity. Figure 6 includes the results of concurrent analyses of cell injury determined via measurements of the surviving fraction as presented in Fig. 5. Thus, at the 10% serum equivalent dose, the ChOx mixture produced a decrease in the surviving fraction that corre-

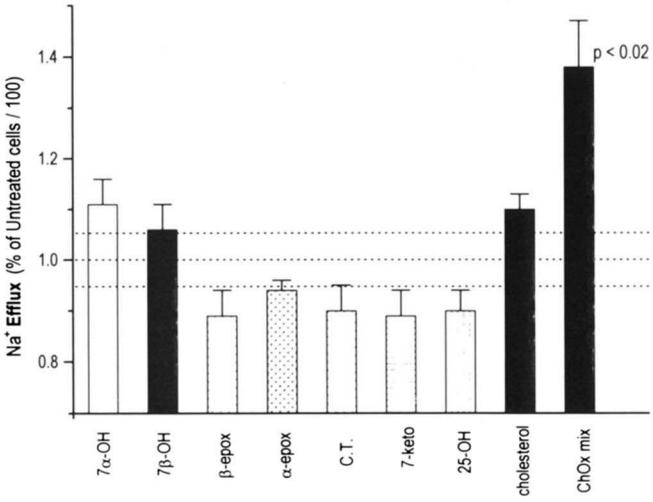

Fig. 7. The effect of individual ChOx and the ChOx mixture of Na^+ efflux from REC. The treatment dose was in each case 0.15 mg/dL (10% serum equivalents). An explanation of serum equivalent dose is found in the Methods and described under Fig. 6. Na^+ efflux was measured after prelabeling REC with $^{22}Na^+$ for 18 h (0.1 μCi/mL in complete medium) prior to addition of ChOx for the final 2 h. The monolayers were then washed three times with choline buffer; Na^+-free buffer was then added to the cells and aliquots were taken for measurement of radioactivity after 5 min. Cell numbers and cell-associated radioactivity were measured at the same time in order to determine the amount of efflux relative to that of cells not treated with ChOx (controls). The results are expressed as a percent of efflux in control cultures. The three dotted horizontal lines indicate the mean and standard error for control cultures. The mean and standard errors from three independent analyses are shown. Determinations of statistical significance were made using one-way ANOVA comparing all treatment conditions to control cultures that were treated with ethanol vehicle (0.2% v/v, ethanol–medium) only. Significant differences from controls are indicated ($P < 0.02$).

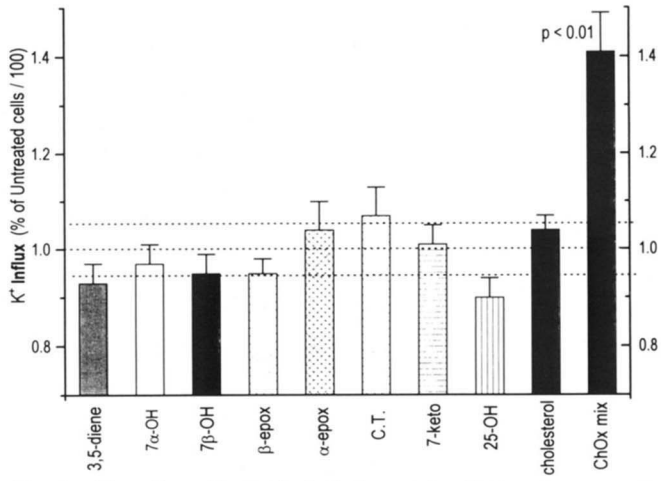

Fig. 8. The effect of individual ChOx and the ChOx mixture on K^+ influx into REC. ^{86}Rb was used as a radiotracer. The treatment dose was in each case 0.15 mg/dL (10% serum equivalents). An explanation of serum equivalent dose is found in the methods and described under Fig. 6. For these studies, REC were grown in 24-well plates and uptake of ^{86}Rb was measured over a 2-h period concurrent with the treatment of the monolayers with the ChOx mixture in DMEM–M199 4:1 and [^{86}Rb]Cl, 1 μCi/ml, (sp act, 4.6 mCi/mmol) containing 2% FBS. At the end of treatment the media were removed and the monolayers were washed three times with PBS containing excess K^+, trypsinized, and counted for cell number and radioactivity. Cell numbers and cell-associated radioactivity were measured in order to determine the amount of influx relative to that of cells not treated with ChOx (controls). The results are expressed as a percent of the control rate of influx. The three dotted horizontal lines indicate the mean and standard error for control cultures. The mean and standard errors from three independent analyses are shown. Determinations of statistical significance were made using one-way ANOVA comparing all treatment conditions to control cultures that were treated with ethanol vehicle (0.2% v/v, ethanol–medium) only. Significant differences from controls are indicated ($P < 0.01$).

sponded to the sharp increase in protein leakage measured as [^{14}C]leucine-derived radioactivity. Using the methods described above, it was noted that none of the phospholipid fractions isolated from LDL, Cu^{2+}-oxidized LDL, or plasma produced a measurable increase in toxicity or [^{14}C]leucine leakage at serum equivalent doses of up to 20% (data not shown).

Cytotoxic characterization of ChOx in previous studies focused on the isomeric cholesterol epoxides, α-epox and β-epox, and their hydration product, 3β,5α,6β-cholestane triol (CT) (21). The geno- versus cyto-toxic effects of these compounds were found to be interrelated; however, the mechanism for cell injury and death appeared to be epigenetic and implicated damage to the cell membrane(s). This was described in other studies wherein various ChOx were found to be incorporated into and altered the structure and permeability of cell membranes (23). Using the cytotoxicity data described above, the effects of individual ChOx and the ChOx mixture on the transport of Na^+, K^+, and Ca^{2+} ions were examined. For these experiments, we used a 10% serum equivalent treatment dose for the individual ChOx or for the total concentration of the ChOx mixture. This corresponds to 10% of the plasma concentration of ChOx as shown in Fig. 4 (i.e., 10% of 1.5 mg/dL or 0.15 mg/dL). A 2-h treatment period in 80/20:DMEM/M199 medium containing 2% heat-inactivated serum resulted in cell survival greater than 85% in all cases. The effects of individual ChOx and the ChOx mixture on Na^+ efflux from REC under these treatment conditions are shown in **Fig. 7.** None of the ChOx or unoxidized cholesterol significantly affected the extent of Na^+ efflux from cells measured over the last 5 min of the 2-h treatment period. In each case, there was a marginal increase or decrease in the extent of efflux as compared to that measured in untreated cells (dotted horizontal lines representing the mean and standard error of the controls). Of the individual ChOx tested, β-epox, 7-keto, and 25-OH produced the most marked inhibition of Na^+ efflux while 7α-OH and cholesterol caused a marginal increase in efflux. On the other hand, the ChOx mix produced a 1.4-times increase in Na^+ efflux ($P < 0.02$). Similar effects were seen for measurements of Na^+ influx measured under the same treatment conditions (data not shown). **Figure 8** shows the effects of ChOx and the ChOx mixture on K^+ influx, measured as the extent of ^{86}Rb influx over the 2-h treatment period. None of the individual ChOx or cholesterol affected the rate of K^+ influx; however, the ChOx mixture produced a significant increase ($P < 0.01$). The extent of this increase matched that found for Na^+ efflux and influx. The stimulatory effect of the ChOx mixture was completely blocked by ouabain at a concentration (0.1 μM) that inhibited K^+ transport by 90% in control cultures, suggesting the involvement of enhanced Na^+/K^+-ATPase in the stimulated rates of Na^+ and K^+ flux. Consequently, the data shown in Figs. 7 and 8 can be regarded as ouabain-sensitive Na^+ and K^+ flux. Pretreatments with 1 mM amiloride also prevented the ChOx-induced Na^+ uptake when ChOx treatment concentrations exceeded 10% serum equivalents (data not shown).

The effects of the ChOx on $[Ca^{2+}]_i$ were also studied. Addition of the ChOx mixture at a 10% serum equivalent concentration (0.15 mg/dL) to REC (maintained in complete medium) produced a rapid increase in the $[Ca^{2+}]_i$ that reached maximum levels that were 175% of the control $[Ca^{2+}]_i$ by 1 h. The $[Ca^{2+}]_i$ then decreased over the following 48 h but remained significantly elevated ($P < 0.05$) over basal levels (**Fig. 9**). Addition of pure cholesterol at a 10% serum equivalent concentration (15 mg/dL) also resulted in a rapid rise in the $[Ca^{2+}]_i$, reaching a maximal 25% increase over baseline and then decreasing to approximately 10% over baseline for the remaining 70-h measurement period. No significant increases in $[Ca^{2+}]_i$ were found after additions of nLDL or LDL at 10% serum equivalent concentrations (data not shown). Microscopic examination of cells revealed morphological changes after ChOx addition over a 24-h period. This was observed previously when CT

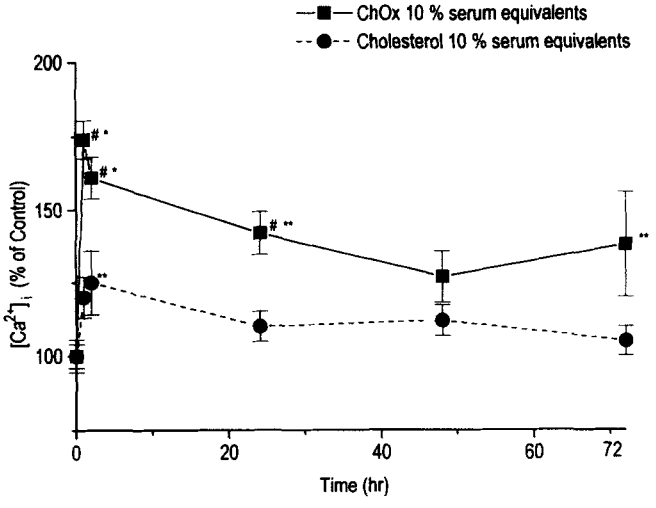

Fig. 9. The effect of the ChOx mixture on the $[Ca^{2+}]_i$ of REC after addition of a 10% serum equivalent concentration (final concentration) of the ChOx mixture (prepared in complete medium containing 2% FBS) to cultures maintained in cuvettes as described under Methods. After addition to the cultures, the fluorescence intensity of fluo-Ca^{2+} complex was measured at designated intervals over a 72-h period. Control cultures were maintained in the DMEM–M199 80:20 containing 2% heat-inactivated FBS for the same period, the measured $[Ca^{2+}]_i$ was arbitrarily set as 100% and used to calculate the increases in $[Ca^{2+}]_i$ due to addition of ChOx which are expressed as a percent of control levels at that interval. Significant increases over controls (which were set at 100% for each time period analyzed) are indicated as: *, $P < 0.01$, and **, $P < 0.05$ as determined using a two-tailed *t*-test. Significant differences between ChOx and cholesterol treated cells are indicated by #, $P < 0.05$. Results shown are the mean and standard errors for three independent analyses.

was added to endothelial cells (37) where changes in the shape and contact between cells were measured. To examine this further, cell size was determined 1 h after addition of the ChOx mixture by trypsinization and measurement of cell numbers and size distribution using a Coulter counter. **Figure 10** compares the changes in cell volume and the maximum $[Ca^{2+}]_i$ measured after addition of the ChOx mixture to REC. A dose-dependent increase in the $[Ca^{2+}]_i$ was found up to a 20% serum equivalent dose. The increased $[Ca^{2+}]_i$ was only found at concentrations equal to or greater than 10% serum equivalent concentrations. Increases in cell volume approximated the maximum levels of $[Ca^{2+}]_i$ measured at each treatment concentration, although no appreciable increases in cell volume were found at treatment doses greater than 10% serum equivalents. This may be due to cell lysis or because cells reached the maximum volumes attainable for these cultures, or to other unknown limiting factors. As the effects of ChOx doses greater than 10% serum equivalents were not tested in detail for parameters such as K^+ or Na^+ flux, and because treatments greater than 15% serum equivalents produced substantial cell death, the relationship between cell volume and intracellular ion concentrations cannot be fully established at this time. Nevertheless, the increases in $[Ca^{2+}]_i$ (or possibly Na^+ levels) may be explained, in part, by an increase in cell volume.

Table 2 shows the results of studies where the cytotoxicity of selected ChOx or the ChOx mixture were compared after treatments in complete medium versus medium containing low calcium concentrations (i.e., 50 μM). Each of the individual ChOx tested produced a dose-dependent decrease in cell survival with the order of potency being: CT > β-epox > 7-keto > α-epox. At doses up to 25 μM, the ChOx mixture was more potent than any individual ChOx, suggesting a synergistic action for the various ChOx. When treatments were performed in Ca^{2+}-deficient medium, there was a substantially decreased toxicity for all the ChOx examined. Indeed, at concentrations that may be considered as physiologically relevant (i.e., 25–40 μM) there was negligible toxicity when treatments were performed in Ca^{2+}-deficient medium. This suggests that much of the ChOx-induced cell injury arises from an influx of extracellular Ca^{2+}, likely due to membrane perturbations.

DISCUSSION

Two interrelated aspects of ChOx toxicity were examined: *1)* identification and quantitation of ChOx found in human plasma, and specifically ChOx found in LDL⁻ or formed by subjecting LDL to Cu^{2+}-induced oxidation; and *2)* the types and amounts of ChOx found in LDL⁻ provided the basis for an investigation of the cytotoxicity of a mixture of the major ChOx representing a potential exposure of vascular tissues in vivo. Analysis of human plasma and LDL has shown that ChOx are commonly encountered and may be present in high concentrations in an oxidatively modified subfraction of LDL which we refer to as LDL⁻. Previous studies have shown that the proportion of LDL⁻ may be as high as 8% of the total LDL (15, 38) and the present findings show that nearly one third of the total LDL ChOx in normocholesterolemic human plasma is associated with LDL⁻. In addition, the plasma ChOx concentration is estimated to be approximately 25 μM based on the samples analyzed in this study. This provided a standard to examine the cytotoxicity of ChOx using a mixture of products normally encountered in plasma at biologically relevant concentrations. When LDL is subjected to oxidation, the ChOx levels increase dramatically and the profile of products resembles that found in LDL⁻. Major products formed include 7β-OH, 7-keto, and β-epox, all of which are known products of free radical-dependent cholesterol oxidation. In particular, β-epox is of importance as it is found in considerable amounts in hypercholesterolemic models of atherosclerosis (18, 32, 39), is present at low concentrations in normocholesterolemic plasma, and is absent in the high cholesterol-containing diets used to produce hyper-

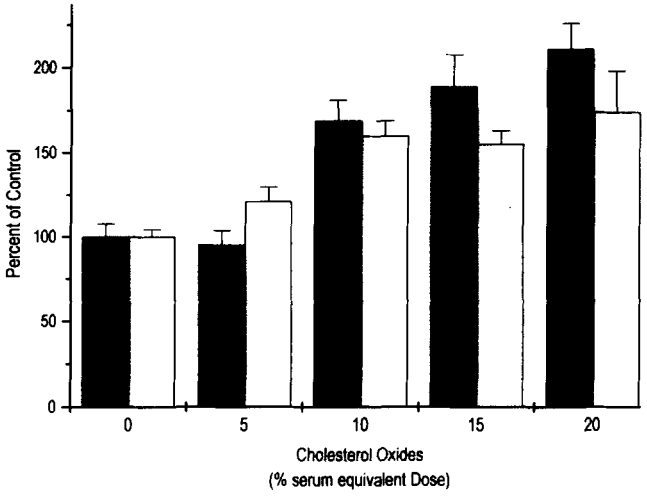

Fig. 10. The concentration-dependent effect of the ChOx mixture on the elevation in $[Ca^{2+}]_i$ and cell volume. Using an average plasma cholesterol level of 150 mg/dL, each 5% serum equivalent incremental dose corresponds to the addition of 0.075 mg/dL ChOx as a mixture. Cell volume (black bars) was determined after trypsinization of the samples by means of the size distribution pattern measured with the Coulter counter. The displayed cell diameters were converted to volume assuming a spherical shape and the reported values are expressed as a percent of the size of untreated (control) cultures, indicated as the zero ChOx treatment dose. The $[Ca^{2+}]_i$ (open bars) represents the maximum $[Ca^{2+}]_i$ measured after addition of the ChOx mixture to the culture. This was usually achieved within 1 h as shown in Fig. 9. The results for each treatment dose are from three independent determinations and are shown as means and standard errors.

cholesterolemia (39). Its formation is inhibited in probucol-treated animals (39), suggesting that it derives from peroxyradical attack of the 5,6-double bond of cholesterol (40). Together with measurements of TBAR and conjugated dienes, formation of ChOx follows the progression of lipid peroxidation in LDL. This can be attributed to the large amounts of cholesterol available for oxidation and its participation in the radical chain reaction. However, unlike polyunsaturated fatty acids, peroxidation of cholesterol is less facile and its primary peroxidation product (cholesterol-7-hydroperoxide) readily decomposes to non-radical products as described previously (17), which essentially terminates the chain reaction. This resembles an "antioxidant effect" proposed by Smith (36) for limiting LDL oxidation as well as other cholesterol-containing lipid systems.

It has been proposed that the oxidizability of LDL bears an inverse relationship to cholesterol content (36, 41). As will be discussed further, Cu^{2+} oxidation of LDL produces considerable amounts of lipid peroxidation products other than ChOx and, in this respect, differs from LDL⁻. Nevertheless, the progression of lipid peroxidation during Cu^{2+}-induced oxidation correlates well with accumulation of ChOx. The variability of LDL to oxidation is well recognized and this also applies to the oxidation of LDL cholesterol. The present findings agree with the general observations of Jialal, Freeman, and Grundy (42), who reported that measurement of oxysterols provides an accurate index of the oxidative modification of LDL. Indeed, among the parameters analyzed for Cu^{2+}-induced LDL modification, the best correlation is between the time-dependent changes in electrophoretic mobility and the formation of oxysterols. However, in contrast to their findings, 7-keto was not the predominant, although it was a major, ChOx in the samples we analyzed. The differences between our findings may be due to the manner by which oxysterols were isolated and analyzed as Jialal et al. (42) subjected the sterol extracts to a harsher saponification procedure and did not convert the sterols to their O-TMS derivatives prior to gas chromatographic analysis.

We used the profile of ChOx found in human plasma for cytotoxicity studies and to compare the effects of ChOx to that of Cu^{2+}-oxidized LDL and LDL⁻. Using

TABLE 2. Effect of Ca^{2+}-deficient medium on ChOx toxicity surviving fraction relative to controls

	Dose[a]			
Compound	5 μM	10 μM	20 μM	40 μM
α-Epox				
$+Ca^{2+}$	1.05 ± 0.02	1.13 ± 0.04	0.69 ± 0.06	0.57 ± 0.07
$-Ca^{2+}$	1.00 ± 0.05	1.25 ± 0.07	1.02 ± 0.05[c]	1.01 ± 0.02[c]
β-Epox				
$+Ca^{2+}$	0.93 ± 0.06	0.77 ± 0.06	0.66 ± 0.08	0.43 ± 0.09
$-Ca^{2+}$	1.15 ± 0.07	1.17 ± 0.11[b]	1.03 ± 0.03[c]	0.91 ± 0.05[c]
CT				
$+Ca^{2+}$	1.14 ± 0.02	0.80 ± 0.09	0.45 ± 0.10	0.05 ± 0.10
$-Ca^{2+}$	1.05 ± 0.08	0.79 ± 0.05	0.76 ± 0.13	0.15 ± 0.11
7-Keto				
$+Ca^{2+}$	1.03 ± 0.05	1.21 ± 0.05	0.78 ± 0.09	0.20 ± 0.06
$-Ca^{2+}$	0.96 ± 0.08	1.11 ± 0.04	1.07 ± 0.10[b]	0.22 ± 0.15
	Dose[d]			
	5%	10%	20%	30%
ChOx mix				
$+Ca^{2+}$	0.85 ± 0.05	0.62 ± 0.13	0.52 ± 0.10	ND
$-Ca^{2+}$	0.96 ± 0.06	0.87 ± 0.08	0.80 ± 0.06[b]	ND

[a]The treatment concentration for individual ChOx is expressed as μM.
[b]$P < 0.05$ comparing $-Ca^{2+}$ versus $+Ca^{2+}$ at the indicated treatment dose as determined by Student's *t*-test.
[c]$P < 0.01$ comparing $-Ca^{2+}$ versus $+Ca^{2+}$ at the indicated treatment dose as determined by Student's *t*-test.
[d]For the ChOx mixture the treatment dose is given as percent serum equivalents where a 10% serum equivalent is approximately 0.15 mg/dL according to the ChOx content shown in Fig. 4.

measurements of cell survival and protein leakage as determinants of injury, we found that neither pure cholesterol nor the phospholipids isolated from oxidized LDL were toxic at levels found in LDL⁻. On the other hand, the ChOx mixture found in LDL⁻ closely replicated the dose–response curve for LDL⁻-induced cytotoxicity. Given the relative absence of other lipid peroxidation products in LDL⁻, it is plausible that the toxic component(s) known to be associated with the lipid fraction (7) are likely the ChOx. The toxicity of LDL⁻ from humans was similar to that of LDL⁻ recovered from monkey plasma as described previously (16). The cytotoxicity of these ChOx has been demonstrated with many vascular cell types, where the effects on smooth muscle cells (SMC) (18, 43) monocyte/macrophages (44), and endothelial cells (21) are particularly relevant. Cytotoxicity to arterial endothelial and SMC likely has significant implications for atherosclerosis as these two cell types play a pivotal role in the etiology of the disease (45). There are many reports describing ChOx cytotoxicity over a wide concentration range (37, 43, 44, 46–48). There is now further evidence that pure (unoxidized) cholesterol when administered at levels found in hypercholesterolemic subjects is not cytotoxic to cultured endothelial cells. Elevated levels of ChOx in hypercholesterolemic and normocholesterolemic individuals represents a future point of interest for the study of atherogenesis that is attributed to cholesterol in general.

The cytotoxic potency of Cu^{2+}-oxidized LDL is likely attributable to other lipid-associated components. This is reasoned on the basis that the ChOx content of LDL⁻ and Cu^{2+}-oxidized LDL are similar (Table 1) yet the latter is nearly twice as toxic, as shown in Fig. 5. The nearly 10-fold greater levels of other lipid peroxidation products (e.g., TBAR and lipid peroxides) may account for the greater margin of toxicity. The aldehydic products of lipid peroxidation, such as 4-hydroxynonenal (6) are known to be highly cytotoxic and appear to be present in relatively low levels in LDL⁻. In this respect, LDL⁻ more closely resembles the peroxide composition of minimally modified LDL that is produced by mild in vitro oxidation (J. Berliner, personal communication).

The vascular endothelium acts as a barrier to ions, lipoproteins, and other plasma components. Injury to endothelium by ChOx may disturb endothelial integrity resulting in alteration of the barrier function of the vascular endothelium allowing increased penetration of these plasma components. It was previously shown that CT increased albumin transfer across endothelial monolayers (49). In addition, increased permeability to Ca^{2+} and rubidium was reported after treating P815 cells (50) or L-cells (24) with 25-OH. Loss of the membrane Ca^{2+} transport function and intracellular Ca^{2+} homeostasis is a mechanism by which many compounds produce cell death (51). In this study we found that the ChOx found in LDL⁻ affect the rate of Na^+, K^+, and Ca^{2+} flux at subtoxic treatment concentrations. At similar concentrations, the individual ChOx minimally affected ionic flux while the ChOx mixture produced a marked increase in the influx (or efflux) of these ions, indicating that a synergistic interaction may take place when all the ChOx are present. When higher doses of ChOx were added, producing greater cytotoxicity (surviving fraction less than 0.7), damage to the membrane was evident by leakage of cell proteins. The effect of the ChOx mixture appears to be more than simply an additive effect of the individual components as levels of cytotoxicity and effects on ion transport were comparable among the individual ChOx but were markedly less than the effect of the mixture at a comparable dose (e.g., Fig. 7). Indeed, none of the ChOx at the levels present in the mixture (≤ 5 μM each) are toxic when administered alone (inferred from data in Table 2).

Our findings suggest that the ChOx perturb membrane structure, and at sublethal doses disrupt the transport of ions. However, this appears not to involve general membrane disruption because the ChOx mixture, at comparable doses, has no effect on glucose transport as measured by the rate of [^{14}C]-2-deoxyglucose uptake (data not shown). This is also indicated by the ouabain-sensitive enhancement of Na^+ and K^+ flux suggesting activation of Na^+/K^+-ATPase. It is also possible that increased K^+ and Na^+ influx may be linked to Ca^{2+} influx where Na^+/Ca^{2+}, K^+/Ca^{2+}, Na^+/H^+, or H^+/Ca^{2+} transporters could be involved when K^+ and Na^+ homeostasis is disrupted, as suggested by the inhibitory effect of amiloride. The effects on ion flux can be explained in terms of the membrane structural changes produced by ChOx (23); however, we could not determine the extent to which increases in $[Ca^{2+}]_i$, or influx of Na^+, are due to passive leakage. This precaution is based on the general permeabilizing effect of the ChOx that is evidenced by cell swelling. Indeed, the changes found for K^+ and Na^+ flux may be explained by a net increase in cell volume. Size distribution analysis using the Coulter counter indicated increased cell volumes corresponding to the changes in K^+/Na^+ flux. However, this cannot account for the changes in $[Ca^{2+}]_i$ suggesting that this effect is driven by specific membrane transport processes that are perturbed by ChOx. Moreover, the marked protection afforded by treatments in Ca^{2+}-deficient medium (Table 2) indicates that much of the cytotoxicity is due to Ca^{2+} influx with prolonged increases in $[Ca^{2+}]_i$ that are known to induce cell death. The contribution of elevated $[Ca^{2+}]_i$ cytotoxicity could not be fully investigated as approaches such as Ca^{2+} buffering or chelation were not possible because cells would not remain viable long enough to perform these experiments. Earlier

studies showed that several ChOx individually altered Ca^{2+} homeostasis by affecting the activity of Ca^{2+} transporters (26).

Reduction or cessation of cell growth of cultured mammalian fibroblasts has been observed after treatments with certain ChOx. The inhibition of DNA synthesis, measured by [^{3}H]thymidine incorporation, correlated with the cytotoxic potencies of several ChOx (52). The cytostatic or cytotoxic effect of the ChOx present in LDL may also be due to the inhibitory action reported for some ChOx on cholesterol synthesis (53), which may deplete isoprenoids and sterols required for cell division and growth. The sterol depleting effect of ChOx may also contribute to the noted perturbations in ion flux (24). The in vivo effects of ChOx administered orally (54–56) or intravenously (19) have been described in terms of vascular injury evidenced by morphologic changes by means of light and electron microscopy. Administration of CT, 25-OH, α-epox, and 7-keto individually to New Zealand white rabbits (19, 54), rats (55), and chicks (19) caused alterations in the aortic wall suggestive of cytotoxic/necrotic processes. In non-human primates, CT and 25-OH induce changes consistent with atherosclerosis. These include arterial wall calcium accumulation, wrinkling of nuclear membranes, nuclear pyknosis, cytoplasmic involution, and endothelial degeneration and desquamation (57, 58). Indeed, all the cholesterol oxidation products described above are derived from the primary peroxidation products of cholesterol, namely 7β-hydroperoxycholest-5-en-3β-ol (cholesterol-7-hydroperoxide) (36, 40). Cholesterol-7-hydroperoxide was recently shown to be a primary cytotoxin in oxidized LDL and was found in human atherosclerotic lesions (59). The cholesterol oxide mixture described in this study could likely mimic the action of cholesterol-7-hydroperoxide on cultured cells through a facile decomposition of the hydroperoxide to the various cholesterol oxidation products, which contribute to the observed cytotoxicity apparently through different mechanisms (20). Effects regarded as cytotoxic may represent an early component of vascular injury which leads to atherosclerotic lesion development, particularly in hyperlipidemic subjects where ChOx concentrations are usually high.

The authors wish to thank Edward Ramos and Nancy Zhang for their technical assistance in performing the cholesterol oxide measurements and for the preparation of LDL and LDL fractions. This study was supported by a grant, ES03466 from the National Institutes of Health and NATO International Collaborative Grant CRG 920513.

Manuscript received 27 February 1995 and in revised form 8 June 1995.

REFERENCES

1. Steinberg, D., S. Parthasarathy, T. E. Carew, J. C. Khoo, and J. L. Witztum. 1989. Beyond cholesterol: modifications of low-density lipoprotein that increase its atherogenicity. *N. Engl. J. Med.* **230:** 915–924.
2. Ylä-Herttuala, S., W. Palinski, M. E. Rosenfeld, S. Parthasarathy, T. E. Carew, S. Butler, J. L. Witztum, and D. Steinberg. 1989. Evidence for the presence of oxidatively modified low density lipoprotein in atherosclerotic lesions. *J. Clin. Invest.* **84:** 1086–1095.
3. Harland, W. A., J. D. Gilbert, G. Steel, and C. J. W. Brooks. 1971. Lipids of human atheroma. *Atherosclerosis.* **13:** 239–246.
4. Björkhem, I., O. Breuer, B. Angelin, and S-Å. Wikström. 1988. Assay of unesterified cholesterol-5,6-epoxide in human serum by isotope dilution mass spectrometry. Levels in the healthy state and in hyperlipoproteinemia. *J. Lipid Res.* **29:** 1031–1038.
5. Yamamoto, Y., and E. Niki. 1989. Presence of cholesteryl ester hydroperoxide in human blood plasma. *Biochem. Biophys. Res. Commun.* **165:** 988–993.
6. Esterbauer, H., G. Jürgens, O. Quehenberger, and E. Koller. 1987. Autoxidation of human low density lipoprotein: loss of polyunsaturated fatty acids and vitamin E and generation of aldehydes. *J. Lipid Res.* **28:** 495–509.
7. Hessler, J. R., D. W. Morel, L. J. Lewis, and G. M. Chisolm. 1983. Lipoprotein oxidation and lipoprotein-induced cytotoxicity. *Arteriosclerosis.* **3:** 215–222.
8. Morel, D. W., P. E. DiCorleto, and G. M. Chisolm. 1984. Endothelial and smooth muscle cells alter low density lipoprotein in vitro by free radical oxidation. *Arteriosclerosis.* **4:** 357–364.
9. Arshad, M. A. Q., S. Bhadra, R. M. Cohen, and T. R. Subbiah. 1991. Plasma lipoprotein peroxidation potential: a test to evaluate individual susceptibility to peroxidation. *Clin. Chem.* **37:** 1756–1758.
10. Rajavashisth, T. B., A. Andalibi, M. C. Teritto, J. A. Berliner, M. Navab, A. M. Fogelman, and A. J. Lusis. 1990. Induction of endothelial cell expression of granulocyte and macrophage colony-stimulation factors by modified low-density lipoproteins. *Nature.* **344:** 254–257.
11. Berliner, J. A., M. C. Territo, A. Sevanian, S. Ramin, J. Kim, B. Bamshad, M. Esterson, and A. M. Fogelman. 1990. Minimally modified LDL stimulates monocyte-endothelial interactions. *J. Clin. Invest.* **85:** 1260–1266.
12. Tagawa, H., H. Tomoike, and M. Nakamura. 1991. Putative mechanisms of the impairment of endothelium-dependent relaxation of the aorta with atheromatous plaque in heritable hyperlipidemic rabbits. *Circ. Res.* **68:** 330–337.
13. Ohara, Y., T. E. Peterson, and D. G. Harrison. 1993. Hypercholesterolemia increases endothelial superoxide anion production. *J. Clin. Invest.* **91:** 2546–2551.
14. Savenkova, M. I., D. M. Mueller, and J. Heinecke. 1994. Tyrosyl radical generated by myeloperoxidase is a physiological catalyst for the initiation of lipid peroxidation in low density lipoprotein. *J. Biol. Chem.* **269:** 20394–20400.
15. Cazzolato, G., P. Avogaro, and G. Bittolo-Bon. 1991. Characterization of a more electronegatively charged LDL subfraction by ion exchange HPLC. *Free Rad. Biol. Med.* **11:** 247–253.
16. Hodis, H. N., D. M. Kramsch, P. Avogaro, G. Bittolo-Bon, G. Cazzolato, J. Hwang, H. Peterson, and A. Sevanian.

1994. Biochemical and cytotoxic characteristics of an in vivo circulating oxidized LDL. *J. Lipid Res.* **35:** 669–677.
17. Sevanian, A., R. Seraglia, P. Traldi, P. Rossato, F. Ursini, and H. N. Hodis. 1994. Analytical approaches to the measurement of plasma cholesterol oxidation products using gas- and high-performance liquid chromatography/mass spectrometry. *Free Rad. Biol. Med.* **17:** 397–410.
18. Hughes, H., B. Mathews, M. L. Lenz, and J. R. Guyton. 1994. Cytotoxicity of oxidized LDL to porcine aortic smooth muscle cells is associated with the oxysterols 7-ketocholesterol and 7-hydroxycholesterol. *Arteriosclerosis.* **14:** 1177–1185.
19. Peng, S. K., C. B. Tayor, J. C. Hill, and R. J. Morin. 1985. Cholesterol oxidation derivatives and arterial endothelial damage. *Atherosclerosis.* **54:** 121–125.
20. Peng, S. K., A. Sevanian, and R. J. Morin. 1992. Cytotoxicity of cholesterol oxides. *In* Biological Effects of Cholesterol Oxides. S. K. Peng and R. J. Morin, editors. CRC Press, Inc., Boca Raton, FL. 147–166.
21. Sevanian, A., J. Berliner, and H. Peterson. 1991. Uptake, metabolism and cytotoxicity of isomeric cholesterol-5,6-epoxides in rabbit aortic endothelial cells. *J. Lipid Res.* **32:** 147–155.
22. Morin, R. J., and S. K. Peng. 1989. Effects of cholesterol oxidation derivatives on cholesterol esterifying and cholesteryl ester hydrolytic enzyme activity of cultured rabbit aortic smooth muscle cells. *Lipids.* **24:** 217–220.
23. Peng, S. K., and R. J. Morin. 1991. Effects of cholesterol oxides on cell membranes. *In* Biological Effects of Cholesterol Oxides. S. K. Peng and R. J. Morin, editors. CRC Press, Inc., Boca Raton FL. 125–146.
24. Chen, H. W., H. J. Heiniger, and A. A. Kandutsch. 1978. Alteration of $^{86}RB^{+}$ influx and efflux following depletion of membrane sterol in L-cells. *J. Biol. Chem.* **253:** 3180–3185.
25. Peng, S. K., J. C. Hill, R. J. Morin, and C. B. Taylor. 1985. Effects of cholesterol oxides on cholesterol metabolism and membrane function. *Proc. Soc. Exp. Biol. Med.* **180:** 126–134.
26. Neyses, L., R. Locher, M. Stimpel, R. Streuli, and W. Vetter. 1985. Stereospecific modulation of the calcium channel in human erythrocytes by cholesterol and its oxidized derivatives. *Biochem. J.* **227:** 105–111.
27. Lipid Research Clinics Program. 1974. Manual of Laboratory Operations: Lipid and Lipoprotein Analysis. National Institutes of Health, Bethesda, MD. DHEW Publication no. NIH 75-628.
28. Lowry, O. H., N. J. Rosebrough, A. L. Farr, and R. J. Randall. 1951. Protein measurement with the Folin phenol reagent. *J. Biol. Chem.* **193:** 265–275.
29. Esterbauer, H., M. Rotheneder, G. Strirgl, G. Waeg, A. Ashy, W. Sattler, and G. Jürgens. 1989. Vitamin E and other lipophilic antioxidants protect LDL against oxidation. *Fat Sci. Technol.* **91:** 316–324.
30. Corongiu, F. P., S. Banni, and M. A. Dessi. 1989. Conjugated dienes detected in tissue lipid extracts by second derivative spectroscopy. *Free. Rad. Biol. Med.* **7:** 183–186.
31. Pacifici, E. H. K., L. L. McLeod, H. Peterson, and A. Sevanian. 1994. Linoleic acid hydroperoxide-induced peroxidation of endothelial cell phospholipids and cytotoxicity. *Free. Rad. Biol. Med.* **17:** 285–295.
32. Hodis, H. N., D. W. Crawford, and A. Sevanian. 1991. Identification and quantification of cholesterol oxides in normocholesterolemic and cholesterol-fed hypercholesterolemic New Zealand white rabbit plasma. *Atherosclerosis.* **89:** 117–126.
33. Tsien, R., and T. Pozzan. 1989. Measurement of cytosolic free Ca^{2+} with Quin-2. *Methods Enzymol.* **172:** 230–262.
34. Esterbauer, H., J. Gebicki, H. Puhl, and G. Jürgens. 1992. The role of lipid peroxidation and antioxidants in oxidative modification of LDL. *Free Rad. Biol. Med.* **13:** 341–390.
35. Bonanome, A., A. Pagnan, S. Biffanti, A. Opportuno, F. Sorgato, A. Dorella, M. Maiorino, and F. Ursini. 1992. Effect of dietary monounsaturated and polyunsaturated fatty acids on the susceptibility of plasma low density lipoproteins to oxidative modification. *Arteriosclerosis.* **12:** 529–533.
36. Smith, L. L. 1991. Another cholesterol hypothesis: cholesterol as antioxidant. *Free Rad. Biol. Med.* **11:** 47–61.
37. Sevanian, A., H. Peterson, and T. A. Coates. 1988. Cytotoxicity of cholesterol oxidation products in bovine and rabbit aortic endothelial cells. Eighth International Symposium on Atherosclerosis, CIC International edition, International Atherosclerosis Society. Rome, Italy, 1988. 103–118.
38. Avogaro, P., G. Bittolo-Bon, and G. Cazzolato. 1988. Presence of modified low density lipoprotein in humans. *Arteriosclerosis.* **8:** 79–87.
39. Hodis, H. N., A. Chauhan, S. Hashimoto, D. W. Crawford, and A. Sevanian. 1992. Probucol reduces plasma and aortic wall oxysterol levels in cholesterol-fed rabbits independently of its plasma cholesterol lowering effect. *Atherosclerosis.* **96:** 125–134.
40. Sevanian, A., and L. L. McLeod. 1987. Cholesterol autoxidation in phospholipid membrane bilayers. *Lipids.* **22:** 627–636.
41. Jonas, A. 1977. Microviscosity of lipid domains in human serum lipoproteins. *Biochim. Biophys. Acta.* **486:** 10–22.
42. Jialal, I., D. A. Freeman, and S. M. Grundy. 1991. Varying susceptibility of different low density lipoproteins to oxidative modification. *Arterioscler. Thromb.* **11:** 482–488.
43. Peng, S. K., P. Tham, C. B. Taylor, and B. Mikkelson. 1979. Cytotoxicity of cholesterol oxidation derivatives on cultured aortic smooth muscle cells and their effect on cholesterol biosynthesis. *Am. J. Clin. Nutr.* **32:** 1033–1042.
44. Baranowski, A., C. W. M. Adams, O. B. High, and D. B. Bowyer. 1982. Connective tissue responses to oxysterols. *Atherosclerosis.* **41:** 255–266.
45. Ross, R. 1986. The pathogenesis of atherosclerosis: an update. *N. Engl. J. Med.* **314:** 488–500.
46. Cox, D. C., K. Comai, and A. L. Goldstein. 1988. Effects of cholesterol and 25-hydroxycholesterol on smooth muscle cell and endothelial cell growth. *Lipids.* **23:** 85–88.
47. Naseem, S. M., and F. P. Heald. 1987. Cytotoxicity of cholesterol oxides and their effects on cholesterol metabolism in cultured human aortic smooth muscle cells. *Biochem. Int.* **14:** 71–84.
48. Hu, B., D. Hin, W. Fan, S. K. Peng, and R. J. Morin. 1991. Effects of cholestanetriol on cytotoxicity and prostacyclin production in cultured rabbit aortic endothelial cells. *Artery.* **18:** 87–98.
49. Hennig, B., and G. A. Boissonneault. 1987. Cholestane-3β,5α,6β-triol decreases barrier function of cultured endothelial cell monolayers. *Atherosclerosis.* **68:** 255–261.
50. Boissonneault, G. A., and H. J. Heiniger. 1985. 25-Hydroxycholesterol-induced elevations in ^{45}Ca uptake: permeability changes in P815 cells. *J. Cell Physiol.* **125:** 471–475.

51. Schanne, F., A. B. Kane, E. E. Young, and J. L. Farber. 1979. Calcium dependence of toxic cell death: a final common pathway. *Science.* **206:** 700–702.
52. Peterson, A. R., H. Peterson, C. P. Spears, J. E. Trosko, and A. Sevanian. 1988. Mutagenic characterization of cholesterol epoxides in Chinese hamster V79 cells. *Mutat. Res.* **203:** 355–366.
53. Morin, R. J., B. Hu, and S. K. Peng. 1991. Effects of cholesterol oxides on cholesterol metabolism. *In* Biological Effects of Cholesterol Oxides. S. K. Peng and R. J. Morin, editors. CRC Press, Boca Raton, FL. 103–124.
54. Imai, H., N. T. Werthessen, C. B. Taylor, and K. T. Lee. 1976. Angiotoxicity and atherosclerosis due to contaminants of U.S.P. grade cholesterol. *Arch. Pathol. Lab. Med.* **100:** 565–572.
55. Matthias, D., C. H. Becker, W. Godicke, R. Schmidt, and K. Ponsold. 1987. Action of cholestane-3,5,6-triol on rats with particular reference to the aorta. *Atherosclerosis.* **63:** 115–124.
56. Toda, T., D. Leszczynski, and F. Kummerow. 1981. Angiotoxic effects of dietary 7-ketocholesterol in chick aorta. *Paroi Arterielle.* **7:** 167–175.
57. Taylor, C. B., S. K. Peng, J. Safarik, B. Kapuscinska, W. Bochenek, and J. Hill. 1983. Experimental atherosclerosis in squirrel monkeys by feeding cholestane-3β-5α,6β-triol. *Fed. Proc.* **42:** 789 (abstract).
58. Peng, S. K., C. B. Taylor, J. Safarik, J. Hill, and B. Mikkelson. 1982. Arteriosclerosis. induced by 25-hydroxycholesterol in squirrel monkeys. *Fed. Proc.* **41:** 452 (abstract).
59. Chisolm, G. M., G. Ma, K. C. Irwin, L. L. Martin, K. G. Gunderson, L. F. Linberg, D. W. Morel, and P. E. Dicorleto. 1994. 7β-Hydroperoxycholest-5-en-3β-ol, a component of human atherosclerotic lesions, is the primary cytotoxin of oxidized human low density lipoprotein. *Proc. Natl. Acad. Sci. USA.* **91:** 11452–11456.